

TEM study of GaN/AlN quantum dots deposited on vicinal silicon

M. Benaissa^{1*}, P. Vennéguès² and F. Semond²

¹ CNRST, Angle Allal Fassi / FAR, B.P. 8027 N.U. , Hay Riad, 10000 Rabat, MAROC

² CRHEA-CNRS, rue Bernard Grégory, 06560 Valbonne, France

* benaissa@cnrst.ma

Transmission electron microscopy was performed to investigate the use of AlN epitaxial films deposited on vicinal Si(111) as templates for the growth of GaN quantum dots. It is found that the substrate vicinality induces both a slight tilt of the AlN (0001) direction with respect to the (111) direction and a step bunching mechanism. As a consequence, a dislocation dragging behavior is observed giving rise to dislocation-free areas well suited for the nucleation of GaN quantum dots. The microstructure of different QD encountered in the GaN/AlN system is also described.

keywords : GaN, quantum dots, dislocation, vicinal substrate, transmission electron microscopy

1. INTRODUCTION

Control and optimization of the radiative and structural properties of single quantum emitters, quantum dots (QDs), is a core issue of present day optical science and technology.^{1,2} Much effort has been devoted to the growth of nitride self-assembled quantum dots. For many applications, a high density of uniform and spatially ordered QDs is desired as, for example, in the realization of QDs based-lasers where the vertical stacking of QDs increases their total density and consequently the gain.^{3,4,5} Such a stacking may also be of great interest for the realization of quantum computation/information processing devices, because of the existence of a strong built-in electric field due to spontaneous and piezoelectric polarization effects.⁶ In the case of gallium nitride (GaN) QDs, they have attracted in the past decade general attention due to their potential in providing highly efficient short-wavelength (ultraviolet) light emitters. This efficiency is attributed to a strong exciton localization in QDs.

When grown using a molecular beam epitaxy (MBE) system, structural and optical properties of GaN QDs strongly depend on growth parameters. Indeed, when aluminum nitride (AlN) acts as a spacer layer, it is believed that the formation of GaN QDs proceeds generally according to the Stranski-Krastanow (SK) growth mode that often applies for heteroepitaxy in systems with lattice mismatch superior to 2% (2.5% in GaN/AlN system). Basically, GaN grows in the layer-by-layer mode in Ga-rich conditions ($\text{Ga/N} > 1$), while in the opposite case ($\text{Ga/N} < 1$), and at a critical thickness, three-

dimensional (3D) QDs develop on top of a remaining wetting layer. In fact, the relief of strain caused by the lattice mismatch between GaN and AlN overcompensates the increase in surface area and thus accounts for the formation of self-assembled QDs. The formation of GaN QDs is therefore strictly linked to both kinetics and strain relaxation. However, when ammonia (NH_3) is used as a nitrogen source (our case), the realization of good quality GaN/AlN QDs has shown a little deviation from the traditionally known SK mode. In order to increase the surface diffusion length and consequently push the epitaxial growth system closer to the elastic and surface energy equilibrium, a growth interruption was needed.⁷ This interruption resulted in an instantaneous 2D-3D transition, giving rise to the fabrication of self assembled GaN QDs, the room-temperature luminescence of which was shown to be successfully tuned from blue to orange depending on the dots size.

Generally, the main drawback of a GaN/AlN system is its high density of structural defects (dislocations) due to the use of foreign substrates which are not adapted in terms of both lattice parameters and chemistry. The density of dislocations in such films is often superior to 10^{10} cm^{-2} and their presence may influence both the nucleation and the physical properties of QDs. It has already been shown that the nucleation of GaN QDs is influenced by the strain field existing around edge-type threading dislocations: QDs are preferentially nucleated on the extensively strained AlN surface regions close to dislocation cores⁸. Even if QDs are efficient to confine carriers, dislocations may play a detrimental role for their physical properties. In fact, in most envisaged

devices (light emitting diodes, lasers, etc.), carriers would first be created outside QDs and then would diffuse towards QDs. Threading dislocations would act as trap centers for carriers preventing an efficient electrical injection. Therefore, for the realization of efficient devices it would be of great interest to grow QDs on dislocation-free regions. The aim of the present article is to use a direct method that help demonstrate the feasibility of growing QDs on defect-free surfaces. Indeed, the use of high-resolution transmission electron microscopy (HRTEM) is revealed to be a powerful technique that allows to obtain quantitative information on the system's structure on an atomic scale.

2. EXPERIMENTAL

The growth of GaN/AlN QDs on vicinal Si(111) (5° misorientation) was carried out in a RIBER Compact 21 MBE system. The misorientation of the Si surface is parallel to $\langle 11\bar{2} \rangle$ direction while Si surface steps are aligned along $\langle 110 \rangle$ axis. An AlN buffer layer was first deposited at 920°C , which was found to be two dimensional using Reflection high-energy electron diffraction (RHEED). The AlN growth proceeds up to a nominal thickness of 400 nm. This is achieved using a very low growth rate ($0.1 \mu\text{m/h}$) and a nucleation temperature of 650°C followed by a rapid ramping to the growth temperature.⁹ A subsequent 2D GaN layer is then deposited on a fully relaxed AlN buffer-layer at a substrate temperature of 790°C , at a growth rate of $1 \mu\text{m/h}$. This GaN 2D strained layer continued up to a thickness of about 9 ML where growth interruption is performed (meaning that both Ga and NH_3 are stopped). At this stage, the RHEED pattern showed an evidence of surface roughness (changes from streaks to spots) reflecting a 2D–3D transition. This gave rise to the formation of the desired GaN QDs. It will be shown later that these QDs leave behind a very thin GaN wetting layer. A second AlN layer (spacer) is deposited afterwards in the same conditions as above up to a thickness of 60 nm. As formerly described, this spacer layer was again followed by a second GaN QDs layer that was leaved on the surface, so that both QD types (buried and surface) can be studied under the same conditions. This type of samples has also the advantage to shed light on the step bunching issue in relationship with the QDs stacking order.

Transmission electron microscopy (TEM) specimens are prepared using conventional sample preparation techniques, involving mechanical thinning followed by ion milling using Ar^+ at 3–5 keV. Thinned specimens are then examined using a JEOL 2010F field emission gun, operated at 200 keV. For the TEM study, a sample with a high density of QDs is intentionally fabricated on a 5° misoriented Si (111) substrate.

3. RESULTS AND DISCUSSION

First of all, the influence of the Si substrate vicinality on the morphology and the orientation of the AlN layer was studied.

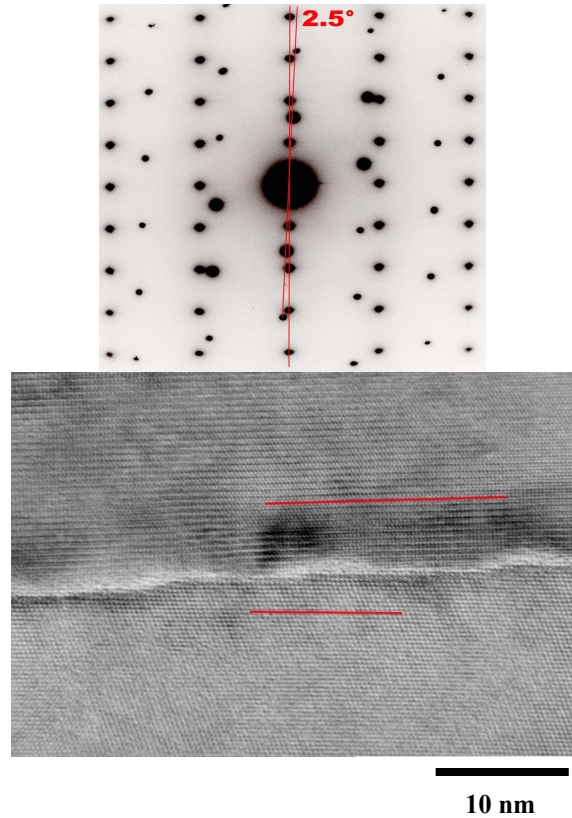


FIG.1 : (a) –top- Selected area diffraction patterns along the Si [1-10] and AlN [11-20] zone axes showing the 2.5° tilt between the Si[111] and the AlN[0001] directions. (b) –bottom- the corresponding HRTEM image viewed along the Si[1-10]. The two lines correspond to the Si(111) and AlN(0002) plans respectively.

Selected area electron diffraction from the Si/AlN interface in cross-section samples along the Si [1-10] zone axis showed a 2.5° disorientation between the Si [111] and the AlN [0001] axes (Fig. 1a). This finding was also confirmed by high-resolution transmission electron microscopy (HRTEM) imaging (Fig. 1b), demonstrating that the AlN growth axis tilt is a consequence of the use of a vicinal Si (111) substrate. In fact, initial AlN growth is supposed to start as atomic incorporations at the edge of Si steps, but also by island nucleation on Si terraces. The two processes thus compete for the arriving atoms particularly when terraces are very narrow such as those in our vicinal Si(111) substrate the width of which is around 10 nm. This competition may suppress the growth of large islands (as it is usually the case in MBE samples) giving rise to a slightly tilted growth front due to the

AlN lateral accommodation upon the edge of Si steps.

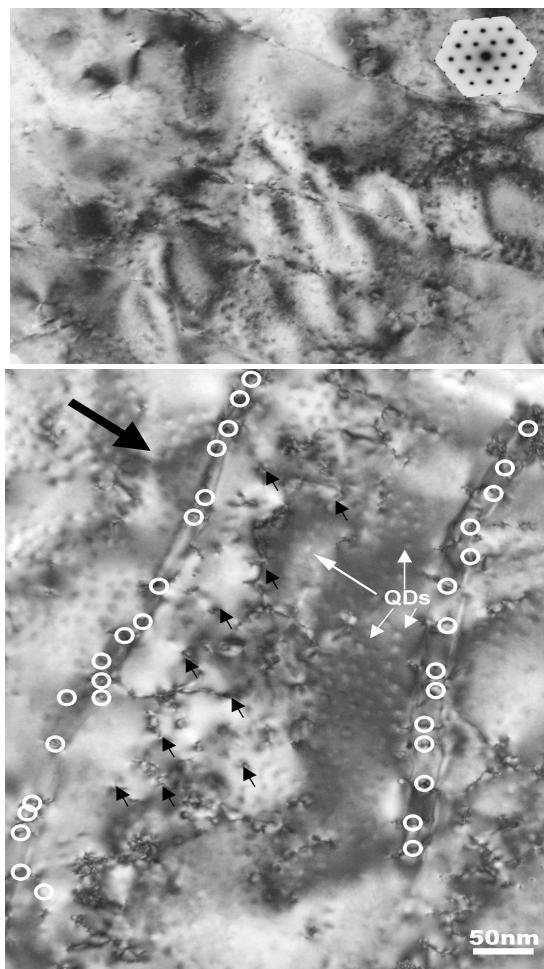


FIG.2 : (a) –top- Bright-field TEM image along a plan-view orientation (AlN [0001] axis). (b) – bottom- The large arrow indicates the macrostep displacement direction. All the dislocations emerging on macrostep edges are shown by white open circles. Small black arrows indicate some dislocations emerging on terraces. White arrows indicate some QDs in both dislocation-free and dislocated areas.

Bright-field TEM imaging along a plan-view orientation (Fig. 2a) reveals the formation of wide macrosteps (150 to 250 nm). This phenomenon, also known as step bunching, is particularly pronounced when the miscut angle of the substrate is high (our case), as it was reported elsewhere.^{10,11,12,13} In fact, the growth of the first AlN thick layer had led to the formation of very high steps, of about 10 nm height (see Fig.3), and large terraces. In other words, our results show that the equilibrium morphology of the vicinal AlN(0001) surface consists of two facets: a large low index facet, AlN(0001), mixed with a high index one in the form of step bunches. It appears therefore that the Si vicinality is partially overcompensated by a slight tilt of the AlN growth direction and by the formation of wide macrosteps.

On the other hand, Fig. 2a illustrates the presence of QDs (dark dots) along edges and onto terraces, with a noticeable contrast corresponding to AlN steps (dark lines), that are aligned parallel to the [11-20] axis, as determined from electron diffraction pattern (see inset). Another revealed feature is the presence of typical threading dislocations contrasts viewed along their lines. To clearly evidence this contrast, plan-view TEM measurements were carried in a two-beams condition with $g=(12-10)$ in which all a -type and $a+c$ -type dislocations are in contrast (Fig. 2b). These measurements elucidated a striking dislocation contrast at the edge of steps, and showed a high dislocation density at these steps as compared to the density measured within terraces. This result suggests that the dislocations were particularly attracted to those parts leaving the other part of the terrace nearly free of dislocations. Further studies using cross-sectional TEM investigations were needed to understand the build-up dislocation network within the AlN film.

On the cross-section TEM image of Fig.3, macrosteps on the AlN surface are clearly visible. The width of the terraces is confirmed and the macrosteps height is estimated to be 8–12 nm. Thanks to the presence of the buried QD plane, the position and the morphology of the AlN surface at an intermediate stage of the growth is revealed. The macrostep edges are evidenced, thanks to the presence of large GaN QDs. Following the position of macrosteps from the buried plane to the surface, it can be seen that the growth occurs both vertically and laterally with a displacement of the macrostep from left to right on Fig. 3 (the dotted line shows the macrostep displacement). From the measurement of the AlN film thickness (between the buried and the surface QD planes) and macrostep edge lateral displacement, the vertical to lateral growth rate ratio is estimated to be equal to 4. Figure 3 corresponds to a very thin TEM specimen and only one dislocation is visible (bold arrow on the left). This dislocation is inclined and passes through successive positions of a macrostep edge. A similar behavior of dislocations has already been observed in AlN layers grown on vicinal sapphire-(0001) substrates.¹⁴

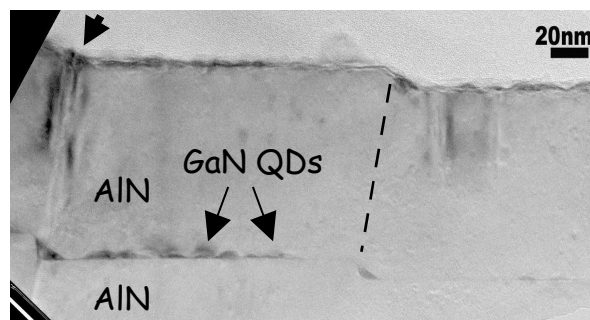


FIG.3 : Cross-section TEM image. Surface and buried QD planes are visible. The dotted line shows

the displacement of a macrostep edge. The black arrow indicates an inclined threading dislocation

Although analyses in a cross section configuration do not give a true image of the dislocation density located at a given edge, since the edge is only viewed along its profile, a series of dark-field TEM images confirmed that the edge of the steps were found to be attractive to dislocation lines within AlN. Figure 4 is a two-beam (1-100) cross-section dark-field image. This orientation is chosen in order to observe the macrosteps edge on. Two kinds of threading dislocations are observed: most of them have a nearly vertical line but a few of them are clearly inclined. These inclined dislocations emerged on the AlN surface at macrostep edges (white arrows). Due to this dislocation inclination, it is important to note that a part of the terraces above the macrostep edges is nearly free of emerging dislocations (horizontal arrows).

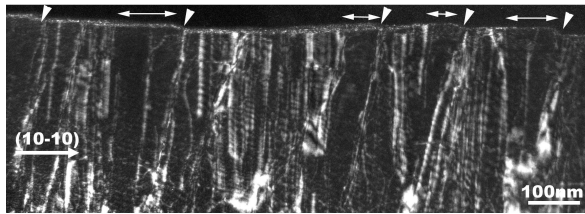


FIG.4 : (10-10) dark-field cross-section TEM image. Inclined dislocations emerge on macrostep edges which are indicated by small inclined arrows. The horizontal arrows show the nearly dislocation-free areas above the macrostep edges.

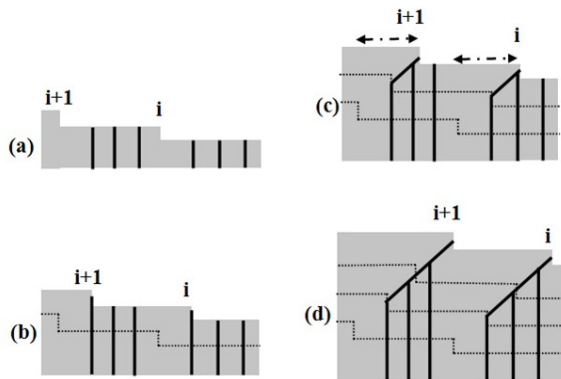


FIG. 5 : Schematic representation of the dislocation bending phenomena. (a) The starting situation is the following: two macrostep edges (i and $i+1$) plus some threading dislocations indicated by vertical lines. (b) Intersection of macrostep edges i and $i+1$ with threading dislocations. The dotted line shows the position of the vicinal surface at the starting point. (c) Intersected dislocations are bent and then they follow the macrostep edges displacement. The horizontal arrows show the dislocation-free areas above the macrostep edges. _d_ Macrostep edge $i+1$

has grown above the starting position of macrostep edge i . All the dislocations are bent and then they emerge on macrostep edges. Terraces are dislocation-free.

The behavior of dislocations can be described as depicted in Fig. 5. We consider a starting situation with an AlN surface formed by macrosteps and with vertical threading dislocations emerging on terraces (Fig. 5a). Due to the lateral displacement of the macrostep edges, they intersect some vertical dislocations (Fig. 5b). At this stage, these dislocations bend and then follow the displacement of macrostep edges, as it is observed in Fig. 3. The area above the bent dislocations is therefore a dislocation-free zone as indicated by arrows in Fig. 5c, where the underneath surface positions are indicated by dotted lines. This situation is what we observed in Fig. 4 in our sample. If the growth proceeds further, we expect that all the vertical threading dislocations intersect a macrostep edge, bend, and therefore emerge in macrostep edges resulting in dislocation-free terraces. This is the case in Fig. 5d, where the macrostep $i+1$ has grown above the first position of the macrostep edge i . However, it seems that in the case of our present sample, the mechanism described in Fig.5 is not complete: the majority of dislocations is still vertical and emerges on the terraces. In fact, macrosteps have only passed through a limited part of the terraces during their lateral displacement. Nevertheless, we already clearly observe dislocation-free areas above macrostep edges where QDs have also nucleated. This result is very promising since one could expect the fabrication of well-suited templates for the growth of QDs. Nonetheless some QDs have still nucleated on surfaces where threading dislocations emerge. White arrows in Fig.2 indicate some QDs nucleated on both kinds of areas. Obtaining fully dislocation-free terraces under our growth conditions and with the same vicinal angle needs the realization of thicker samples where macrosteps during their lateral displacement should pass through the entire terraces. However, because of the large thermal mismatch between AlN and Si, thick AlN films are drastically cracked. Higher vicinal angles result in the formation of narrower terraces. Another way of resolving this issue is to increase the lateral growth rate. Indeed, the lateral growth rate seems to be four times slower than that of the vertical one, as can easily be deduced from ratio measurements of the step-progress to the spacer-thickness (Fig. 3). This means that in order for a macrostep to intercept all threading dislocations, the AlN layer dimension (thickness) must be four times that of the terrace (width), implying that this dislocation dragging behavior will not concern all threading dislocations, which is in full agreement with dislocations densities measured within terraces and at the edge of the steps (as deduced from our plan-view TEM images). The

increase of the lateral growth rate would consequently lead to thin AlN films having large terraces where all threading dislocations are bent and emerge at macrostep edges.

Let's focus now our study on the microstructure of GaN QDs. It is worth mentioning that a preferential nucleation of GaN at the edge of the steps is now clearly evidenced since such a location (either buried or surface) is always occupied by GaN (as shown in Figure 3).

As far as the QDs shape is concerned, three types were distinguished. While surface QDs tend to exhibit a pyramidal shape (Figure 6a), buried ones show typical truncated pyramidal forms (Figure 6b). Indeed, the cross-sectional HRTEM image of Fig. 6b observed along the [11-20] direction depicts a typical GaN QD embedded in the AlN matrix. The wetting layer aside the QD is also visible. By analyzing HRTEM images, the dots are found to present a truncated pyramidal shape with walls inclined by 30° from the surface plane, corresponding to the usual $\{101-3\}$ facets. The average height and base diameter are about 3 nm and 10 nm, respectively. Besides, GaN QDs at the edge of AlN steps show a rather complex form (Figure 6c). It is worth mentioning at this stage that our previous atomic force microscopy study¹⁵ showed that the edges of these steps are saturated with GaN QDs in the form of a chain-aligned GaN QDs, or quantum wires, which are simply the result of a QDs coalescence. It can probably be deduced from this observation that a preference for a nucleation site all along the steps occurred up to saturation. A close examination of such a form shows a complex surface section, which in part is a reproduction of the AlN step edge. This complex shape is evidently due to the fact that step bunches do not form a well defined facet, but rather a multifaceted surface, as clearly shown in Fig.6c. Since all these features were also reproduced on the AlN spacer layer surface, it may therefore be deduced that this capacity to reproduce the morphology of AlN layers might lead to the growth of uniform vertically correlated GaN QDs, provided the density of dots is controlled, either, through the optimization of the adatom diffusion length, or, through the reduction of the terraces' width.

4. CONCLUSION

In summary, we have shown that AlN epitaxial films grown on vicinal Si(111) substrates may be very suitable for the growth of QDs. It was found that the consequence of the Si vicinality is both a slight tilt of the AlN (0001) direction and the occurrence of step bunching. The lateral displacement of macrosteps results in the bending of threading dislocations. Once bent, the threading dislocations emerge on macrostep edges and

therefore terraces above them become free of dislocation providing very suitable templates for the growth of QDs because interferences with structural defects will be prevented. Such templates can also

be explored to enhance the physical properties of AlN films. Up to now, an incomplete process with only a part of the terraces free of dislocation has been obtained. Analyses of HRTEM images performed on the buried dots showed a truncated pyramidal shape with the average height and base diameter of about 3 nm and 10 nm, respectively. Currently a strain distribution study within GaN dots and the AlN spacer layer is under progress and will be published elsewhere.

Acknowledgements

Two of the authors (M.B. and P.V.) acknowledge the partial support from the CNRST-(Morocco) /CNRS-(France) convention SPM No. 17789.

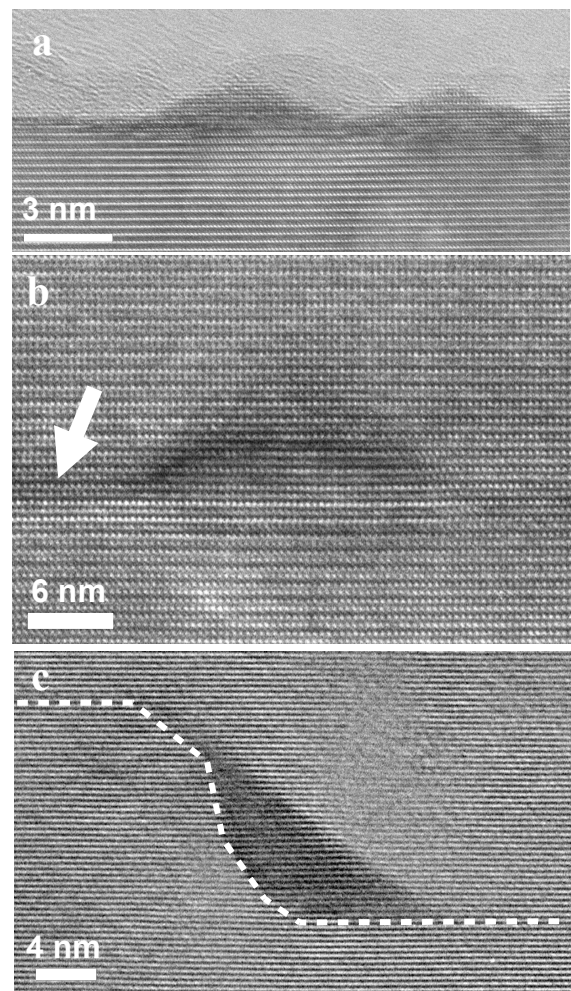


FIG.6 : HRTEM images of GaN/AlN QDs. (a) a surface QD exhibiting a pyramidal shape, (b) a buried QD showing a truncated shape, and (c) a typical QD located at the edge of an AlN step

1. P. Michler, A. Kiraz, C. Becher, W.V. Schoenfeld, P.M. Petroff, Lidong Zhang, E. Hu, and A. Imamoglu, *Science* **290**, 2282 (2000)
2. J. N. Farahani, D.W. Pohl, H.-J. Eisler, and B. Hecht, *Phys.Rev.Lett.* **95**, 017402 (2005)
3. B. Daudin, F. Widmann, G. Feuillet, Y. Samson, M. Arlery, and J. L. Rouvière, *Phys. Rev. B* **56**, R7069 (1997)
4. K. Tachibana, T. Someya, and Y. Arakawa, *Appl. Phys. Lett.* **75**, 2605 (1999)
5. K. Hoshino, S. Kako, and Y. Arakawa, *App.Phys.Lett.* **85**, 1262 (2004)
6. S. De Rinaldis, I. D'Amico, E. Biolatti, R. Rinaldi, R. Cingolani, and F. Rossi, *Phys. Rev. B* **65**, 081309(R) (2002)
7. B. Damilano, N. Grandjean, F. Semond, J. Massies, and M. Leroux, *Appl. Phys. Lett.* **75**, 962 (1999)
8. J. L. Rouvière, J. Simon, N. Pelekanos, B. Daudin, and G. Feuillet, *Appl. Phys. Lett.* **75**, 2632 (1999)
9. F. Semond, Y. Cordier, N. Grandjean, F. Natali, B. Damilano, S. Vézian, and J. Massies, *phys. stat. sol. (a)* **188**, n°2, 501 (2001)
10. J. Tersoff, Y. H. Phang, Z. Zhang, and M. G. Lagally, *Phys. Rev. Lett.* **75**, 2730 (1995); F. Liu, J. Tersoff, and M. G. Lagally, *ibid.* **80**, 1268 (1998)
11. J. Y. Tsao, *Materials Fundamentals of Molecular Beam Epitaxy* (Academic, Boston, 1993), Chap. 6.
12. M. V. Ramana Murty, P. Fini, G. B. Stephenson, Carol Thompson, J. A. Eastman, A. Munkholm, O. Auciello, R. Jothilingam, S. P. DenBaars, and J. S. Speck, *Phys. Rev. B* **62**, R10661 (2000)
13. J. Brault, S. Tanaka, E. Sarigiannidou, J.-L. Rouvière, B. Daudin, G. Feuillet, and H. Nakagawa, *J. App. Phys.* **93**, 3108 (2003)
14. X. Q. Shen, H. Okumura, H. Matsuhata, *App. Phys. Lett.* **87**, 101910 (2005)
15. M. Benaissa, P. Vennéguès, O. Tottereau, L. Nguyen, and F. Semond, *App. Phys. Lett.* **89**, 231903 (2006)

1
2
3
4
5
6
7
8
9
10
11
12
13
14
15